Noise control strategies using composite porous materials – Simulations and experimental validations on plate/cavity systems

François-Xavier Bécot[a)], Luc Jaouen[b)] and Franck Sgard[c)]

(Received: 1 February 2011; Revised: 30 May 2011; Accepted: 30 May 2011)

This paper examines the potential of using composite porous materials to design robust noise control packages. Composite porous are meso-perforated porous materials in which perforations are filled with another porous material. The work presented here shows that the association of two carefully selected materials could lead to interesting combined properties of sound absorption and sound insulation. A canonical plate/cavity system excited with an internal acoustic source is chosen to illustrate the potential of these materials for noise enclosures. The coupled problem is solved using Finite Element Method. The sound propagation in composite porous materials is described by Biot-Allard's poroelasticity equations. Noise reductions obtained using composite porous are compared to those obtained using homogeneous materials. The sound powers dissipated into the system are also examined to give further insights into the physics of the involved phenomena. The results show that the achieved performances take full benefit of the efficiencies of either materials which form the composite porous for different frequency ranges © ***2011 Institute of Noise Control Engineering*****.**

Primary subject classification: 35.2.5; Secondary subject classification: 75.3

1 INTRODUCTION

To combine sound absorption and sound insulation, enclosures are often treated with poroelastic materials. This kind of sound package has the advantage of being light, usually easily replaceable, but has the strong drawback to exhibit weak performances at low frequencies, both for sound absorption and insulation. To overcome this weakness, it has been shown theoretically[1] and experimentally[2] that the concept of double porosity could be used to increase the absorption performances at low frequencies. This concept, used empirically for decades in acoustic suspended ceilings[3], consists in adding a second network of porosity using e.g. perforations, to the initial microscopic scale of the porous substrate. However, sound insulation properties of these perforated porous materials are very low and limit the overall efficiency of this kind of treatment, as shown experimentally in this paper.

Based on the fact that the influence of the double porosity mainly depends on the permeability contrast between the substrate material and the material contained in the perforations, it has been suggested recently to fill the perforations with another porous material to achieve a so-called "composite porous" material[4,5]. These results, obtained using an analytical model, show that an interesting compromise could be achieved by increasing the absorption and limiting the loss of sound insulation due to the presence of the perforations. Based on these advances, the work presented here proposes to examine the application of these type of solutions to optimize sound package of an enclosure surrounding a sound source.

The overall objective of the present study is to decrease the sound power which is radiated outside the enclosure. It is chosen to focus on the low frequency range, namely up to 600 Hz, where porous materials present low performances. The results presented here follow those presented in Ref. 6 which were mainly numerical. Some of the experimental results have also been presented in Ref. 7.

The paper is organized as follows. The studied system and the corresponding model are presented in the next two sections. The materials and the experimental setup designed to illustrate the concepts discussed here are then described. Finally the simulation results

[a)] MATELYS, Acoustique and Vibrations, 1 rue L. et M-L. Baumer, 69120 Vaulx-en-Velin FRANCE; email: francois-xavier.becot@matelys.com.
[b)] MATELYS, Acoustique and Vibrations, 1 rue L. et M-L. Baumer, 69120 Vaulx-en-Velin FRANCE.
[c)] IRSST (Institut de recherche Robert-Sauvé en santé et en sécurité du travail), Service de la recherche, 505, Boulevard de Maisonneuve Ouest, Montréal, (Québec) H3A 3C2 CANADA.

together with experimental data are reported and discussed. Some conclusions are drawn on the relevance of these concepts to design robust noise control solutions.

2 DESCRIPTION OF THE STUDIED SYSTEM

The system studied in this paper consists of a rigid walled cavity which is coupled to a flexible plate. The dimensions are indicated in Fig. 1. A 2 mm thick aluminum plate is embedded in a rigid baffle of infinite dimensions and is supposed to be simply supported. The plate is assumed to radiate sound in the semi-infinite space without being loaded by the exterior surrounding air. The plate is coupled to the fluid enclosed in the cavity which is supposed to be air at rest, at ambient conditions of temperature and pressure. In the absence of sound package, dissipation is included in air to avoid infinite resonances using a structural loss factor of 0.1%. The cavity is parallelepipedic and all 5 walls are acoustically rigid. This means that any sound transmitted through the cavity walls which could be measured in front of the plate is omitted. The system is excited using a harmonic monopole point source placed close to a corner facing the flexible plate (see Fig. 1). With this source position, all modes of rigid walled cavity have the same probability to be excited by the source.

Numerical results presented in Ref. 6 show that the base system without treatment exhibit two different behaviors depending on the frequency range considered. At low frequencies and up to 200 Hz, the power radiated by the plate/cavity system is mainly governed by the modes associated with the in vacuo plate. At higher frequencies and in the limit of the frequency range observed in this work, i.e. 600 Hz, the noise radiation is mainly driven by the modes of the rigid walled cavity. According to these results, two different strategies can be thought of to reduce the sound power radiated outside the enclosure.

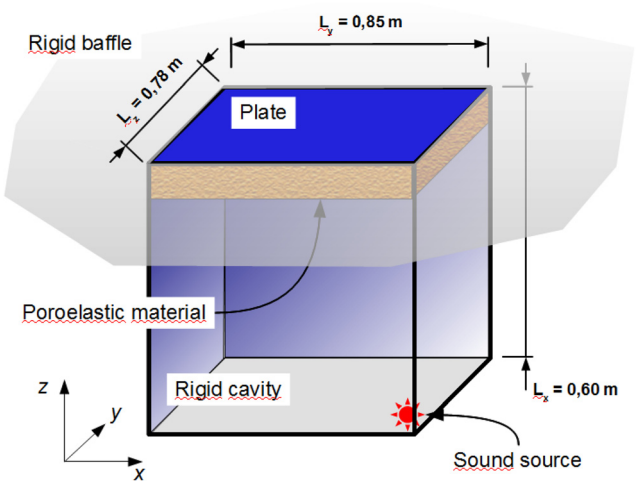

Fig. 1—Scheme of the plate/cavity system used in the numerical simulations and the experiments.

The first strategy is to increase the sound absorption inside the cavity. In this case, a porous slab is laid directly against a cavity rigid wall. This strategy will be mainly efficient in the frequency range driven by the rigid wall cavity modes, i.e. above 200 Hz. The second strategy is to apply the material in front of the plate in order both to increase the sound absorption and to reduce the sound transmitted by the plate outside the system. In second scenario, the efficiency of the sound package is expected to show on the entire frequency range of the study. When the plate is treated, two situations may be found: there is an air gap between the porous material and the plate ("unbonded" configuration) or the porous material is directly bonded onto the plate (continuity of all displacements and stresses). This means that in the first configuration, the porous frame is not directly coupled to the plate whereas in the second case it is. It should also be noted that the presence of the poroelastic material inside the cavity leads to a reduction of the volume available for air, thus leading to a modification of the cavity modes.

In the present work, only the strategy where the treatment is placed in front of the plate is considered. This corresponds indeed to the interesting feature of composite porous materials which could combine both sound absorption and insulation enhanced properties. In addition, for numerical reasons explained later, only the "unbonded" configuration is examined.

The performance of the sound package is assessed in terms of the values of the sound power radiated by the plate outside the system. In the following, the power dissipated in the different components of the system is also discussed to explain some results.

3 MODELING OF THE SYSTEM

The model used in the present study is fully described in Ref. 6. Therefore, only the information which is relevant to the calculations presented here is given. Since the main effort of the present study concerns the development of an innovative porous treatment, a larger part is dedicated here to the modeling of the porous materials.

3.1 Modeling of the Porous Treatment: Five Approaches

In total five approaches have been used to represent the porous material inside the plate/cavity system depending on the mounting conditions or on the dissipative effects which are sought.

The first model arises from the finite element discretization of the ($\underline{u}, p$) formulation of Biot's poroelasticity equations as derived in Ref. 8. In this representation, $\underline{u}$ is the vector of the porous skeleton displacements and p is the scalar interstitial pressure of the fluid contained in the pores. In this representation, the porous material is assumed to be homogeneous at a macroscopic scale, i.e. the wavelength of the impinging sound is large compared to the elementary representative volume dimensions of the porous medium. The sound propagation is described using two coupled equations, one for the porous skeleton phase and one for the fluid phase, and solved using a weak integral form (see for instance Ref. 8). This model will be called "poroelastic". This model is considered as the more complete model in our case since all possible dissipation mechanisms are included: visco-inertial and thermal effects in the fluid phase, and the structural effects due to the deformation of the porous frame.

In the second and third models, the deformations of the porous material skeleton are not considered. These approaches are valid when the deformation of the material skeleton can be neglected or the associated inertial forces dominate the elastic ones. Dissipation in the system is then only due to visco-inertial and thermal effects. The second model considers that the skeleton is rigid and motionless ("motionless frame" model), the third one considers that the skeleton has no stiffness ("limp" model)[9,10]. Another model, called "rigid body" model and which considers that the skeleton is motionless but can move as a whole, was not implemented here because it is equivalent to the "limp" model for materials having a porosity close to 1[6]. In these approaches, the material behavior is solely described using the interstitial fluid pressure p. Therefore, these models may be relevant to represent the treatments of the rigid walls and of the flexible plate, provided that the material is not in direct contact with the plate[6].

In the fifth approach, the presence of the poroelastic material in the system is accounted for using a locally reacting impedance boundary condition on the cavity walls ("impedance" model). This approach is the less computationally demanding and gives similar results to the "motionless frame" model in the case when the treatment is applied to the walls of the cavity[6,11].

Due to formatting restrictions, only the "poroelastic" model has been used in the simulations presented in the following. Interested readers are referred to the above references for discussion on the different models of porous materials.

3.2 Assembling the Different Parts of the System

In the finite element implementation of the complete model of the plate/cavity system, the motions of the plate are modeled using a standard displacement formulation and the air inside the cavity satisfies the Helmholtz equation. Note that the plate damping is accounted for using a structural loss factor. The plate Young's modulus is therefore assumed to be complex valued.

The weak integral forms associated with these equations are derived and directly discretized using finite elements. For the plate, four nodes shell elements are used. For the air inside the cavity and for the "poroelastic" elements, 8 noded brick elements are used. The entire system is finally assembled using the appropriate coupling conditions as described in Ref. 12. In order to reduce the size of the working matrices, two different forms of the ($\underline{u}, p$) poroelasticity equations may be used depending on the nature of the adjacent elements as described in Ref. 13.

The mesh size of the finite element model depends on the modal contents of the different components in the frequency range of interest. Up to 600 Hz, the highest mode is (8,8) for the stand alone plate in the (x,y) plane and (2,2,2) for the rigid walled cavity. On the basis of a 6 elements per wavelength criterion, the final mesh is set to contain 24 elements in both the x- and the y-directions. For the cavity, the mesh is extruded along the z-direction, which means that 24 elements are also used in the x- and y-directions. The number of elements imposed by the highest mode along the z-direction would not exceed 6. However, an oversized mesh containing 21 elements is chosen in order to be consistent with the other two directions. When the poroelastic material is placed in front of the plate, 8 finite elements are taken along the material thickness in the z-direction. For this configuration, a typical finite element model contains slightly more than 17,000 elements for over 32,000 degrees of freedom.

It is worth mentioning that the implementation of the finite element model without sound package has been validated by comparison with a modal analytical approach. In the absence of the poroelastic treatment, this approach may be numerically interesting since the cavity and the plate are only weakly coupled at low frequencies and that the number of modes to be included is low. However, this approach may be too restrictive to accurately represent situations where the material is placed in front of the plate and has not been examined in the present study.

4 THE TESTED MATERIALS: CHARACTERIZATION AND MODELING

For the numerical simulations presented here, three different materials have been used. Two materials are

semi-closed cell foams and one is an open cell foam. These are the base materials referred to as single porosity materials. In addition, these materials have been used in combination with each other to illustrate the potential of composite porous materials.

4.1 Base Porous Materials – Single Porosity Materials

In order to provide the parameter values which are needed for the implementation of the models, a full acoustical characterization has been carried out on these materials. This procedure, fully described elsewhere[14–16], consists in determining the values of the parameters of the Johnson-Champoux-Allard-Lafarge model[17–19] from impedance tube acoustic measurements.

The operation requires the prior knowledge of the open porosity ϕ and of the static air flow resistivity σ. These quantities are directly measured on dedicated test rigs, following the work described in Ref. 20 for the porosity and the corresponding standard[21] for the air flow resistivity. In addition to these two quantities, the four parameters determined using this procedure are: the high frequency limit of the dynamic tortuosity, α_∞, the viscous and thermal characteristic lengths, respectively Λ and Λ', and the static thermal permeability k_0'. It should be underlined that the method used here is not based on a curve fitting. Each value of the above parameters is determined as a function of frequency using an analytical expression issued from the real and imaginary parts of the dynamic mass density and of the dynamic bulk modulus[22]. The parameter values finally kept are average values in frequency ranges over which the assumption of a rigid frame porous material is valid.

The characterized values of the Johnson-Champoux-Allard-Lafarge model are reported in Table 1. The MEL material is a gray Melamine foam. SC1 and SC2 are semi-closed cell foams and represent very low permeability materials. In the case of SC1 which exhibits a very high resistivity value, the five parameters' Johnson-Champoux-Allard model appeared to be more adapted and the value of k_0' has not been determined. Semi-closed cells have been chosen here because they are mainly used for their sound insulation properties and thus present an interesting complement to purely absorbing materials like MEL.

In addition, in order to obtain the input parameters for the "poroelastic" model, the elastic and damping parameters have been characterized using a procedure inspired from the work presented in Ref. 23 and further modified in Ref. 24.

The basic idea of this method is to reproduce a mass/spring system where the mass is prescribed and the spring is represented by the porous material, further assumed to be isotropic. Using charts of pre-computed results of the system response for different values of stiffness, the apparent Young's modulus E_{app} of the spring, that is of the porous material, is identified. For fibrous materials, that is having a Poisson's ratio equal or close to zero, E_{app} corresponds to the "true" Young's modulus E. However for non-fibrous materials, E_{app} depends on the value of the Poisson's ratio ν of the tested sample. By testing several samples having different shape factors, the "true" Young's modulus and the Poisson's ratio can be determined. In the present study, brick-like samples of different thicknesses have been used. Finally the volumic mass has been directly measured using an electronic weighing machine with precision 0.01 g. The obtained parameters are summarized in the Table 2.

4.2 Concept of Composite Porous Materials

In addition to "single porosity" materials, "composite porous" materials have been considered. "Composite porous" materials are an increment of "double porosity" materials where the perforations are filled with a second porous material, the "client", different from the substrate material, called the "host"[4,5]. The concept of double porosity material has been largely explained in the last few years and interested readers are referred to Ref. 1 for the analytical derivation of the theory and to Refs. 2, 3 and 25 for illustrating applications. As for double porosity materials, depending on the pair host/client, the sound absorption coefficient of composite porous materials may be increased significantly in the low to medium

Table 1—Values of the acoustic parameters of the tested materials. Parameters are either directly measured ("Dir. meas.) or characterized (Charac.).

Method *Parameter*	Dir. meas. ϕ	Dir. meas. σ	Charac. α_∞	Charac. Λ	Charac. Λ'	Charac. k_0'
MEL	0.98	15 500	1.01	100	223	27
SC1	0.92	3 433 800	1.30	0.7	1	–
SC2	0.93	371 600	3.31	18	804	73
Units	–	(N.s.m^{-4})	–	(μm)	(μm)	(10^{-10}m^2)

Table 2—Values of the elastic and damping parameters of the tested materials.

Parameter	E	η	ν	ρ_1
MEL	200 000	0.10	0.44	11
SC1	47 400	0.35	0.49	54
SC2	150 000	0.10	0.40	78
Units	(Pa)	–	–	($kg.m^{-3}$)

frequency range compared to single porosity materials. Accordingly, the main influencing parameters are the meso-porosity of the material defined as the rate of inclusion of the client material, and the permeability contrast between the host and the client materials. To cope with this latter criterion, two different materials were considered in the present study: SC1 or SC2 with MEL inclusions. All materials, single porosity or composite porous materials, were considered having a thickness of 80 mm.

5 PATTERN DESIGN OF COMPOSITE POROUS MATERIALS

In this section, the optimal pattern of the porous composite materials is designed in order to achieve enhanced combined sound absorption and transmission properties. From a modeling point of view, an analytical model has been presented in Refs. 4 and 5 which is more suitable for parametrical studies than the finite element model, more computationally demanding. However the analytical model assumes that the porous frame is rigid and motion less, assumption which is irrelevant for sound transmission problems. Therefore, it is chosen to use the analytical model for the optimization of the sound absorption properties and the finite element model for the optimization of the sound transmission properties.

The analytical model relies on the description of sound propagation in double porosity materials as derived in Ref. 1 where the expressions of the total porosity and of the total permeability make use of a mixing law to account for the porosity of the "client" material[4,5]. The validity of this approach was demonstrated on the basis of comparisons with experimental sound absorption data obtained in impedance tube for several composite porous materials.

To assess the design, the kept indicators are the sound absorption coefficient (SAC) and the sound transmission loss (STL-n) for plane waves under normal incidence. One could note that these indicators correspond to impedance tube test conditions according to ISO 10534-2[26].

The thickness of the material is set to 8 cm, made of two layers of 4 cm (see also Sec. 7.1). In this study, only periodic rectangular lattice of rectangular perforations were considered (see Ref. 2, Fig. 3-right for similar perforation pattern). Thus, the two main parameters of the design were the side length of the perforation L_p and the perforation rate φ_p, also called meso-porosity and defined as $\varphi_p = L_p^2 / L^2$ where L is the size of the lattice, which also corresponds to the period of the pattern (see Fig. 2). Moreover, when the poroelastic material is placed in front of the plate, the computational resources limitations impose that the perforation size fits the size of one element in the x- and y-direction. In this framework, the parametric study showed that, for the two "composite porous" SC1+MEL and SC2+MEL and for the frequency range considered here, the optimal pattern is found for a meso-porosity of 50%.

Figures 3 and 4 compare the values of the indicators SAC and STL-n for single porosity materials to those obtained for composite porous materials. These simulations were obtained using the analytical model for the absorption results[4,5] and a poroelastic model implemented with finite elements as described above for the transmission results. As a reminder, the analytical model used for SAC simulation is based on a mixing law which allows to compute the permeability and the bulk modulus of the composite porous from the corresponding properties of the host and of the client materials. For this latter indicator, sliding boundary conditions were assumed on the sample perimeter. In these figures, the frequency range colored in gray lies above the upper

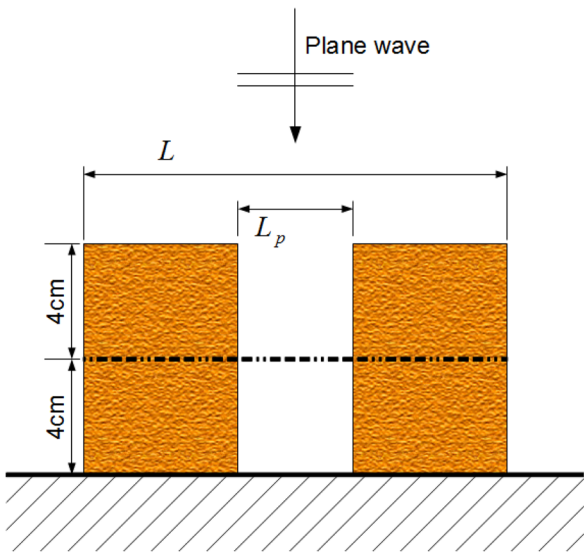

Fig. 2—Side view of the perforated porous material. Absorption configuration: The porous material is backed by a rigid termination.

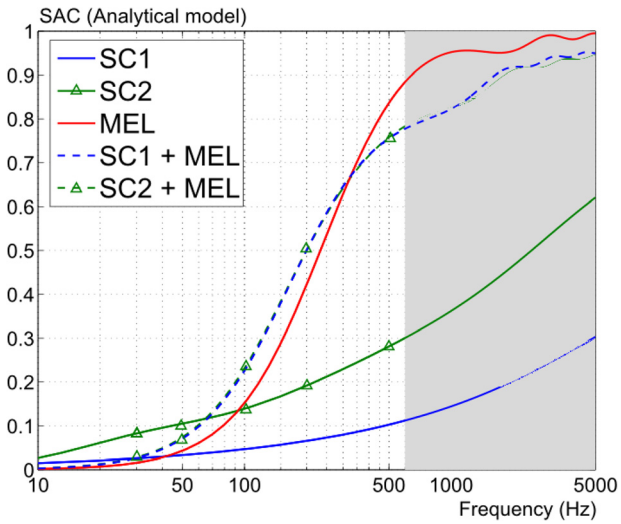

Fig. 3—Sound absorption coefficient (SAC) of single porosity materials and composite porous materials. Simulated data. Conditions of plane wave under normal incidence.

frequency of interest of the present study, namely 600 Hz, but is shown here for the sake of completeness.

As far as single porosity materials are concerned, as expected, the sound absorption coefficients of the semi-closed cell foams SC1 and SC2 are low and do not exceed 0.3 at 600 Hz and 0.6 at 5 000 Hz. Instead, the open cell foam MEL exhibits interesting absorption properties at all frequencies. Concerning the sound

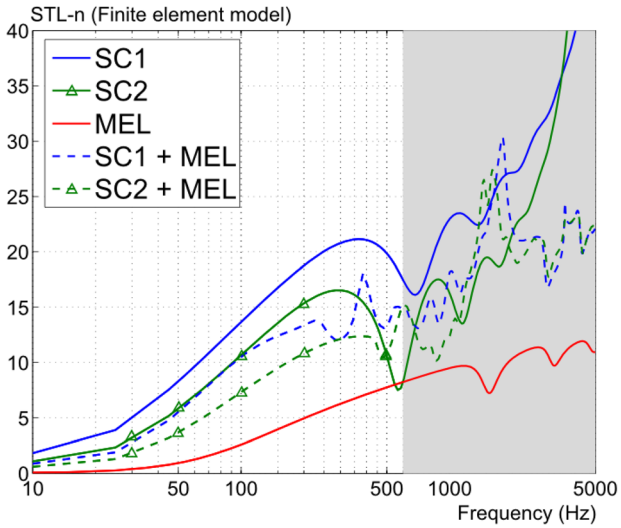

Fig. 4—Sound transmission loss (STL-n) of single porosity materials and composite porous materials. Simulated data. Conditions of plane wave under normal incidence.

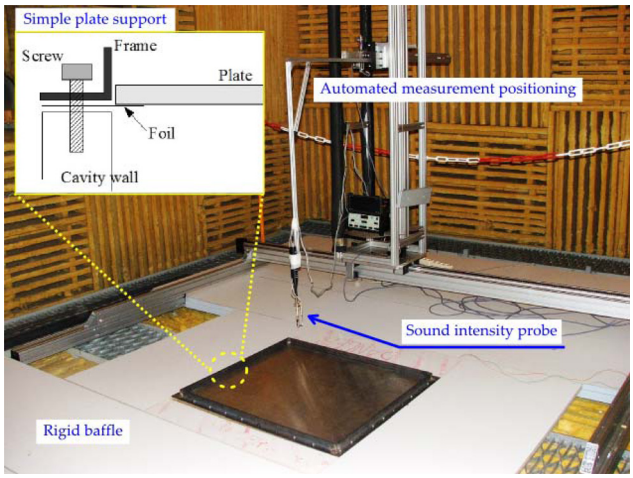

Fig. 5—Picture of the experimental setup and insert of details of the plate simple support (upper left). The face of the plate which radiates outside the system is visible while the below cavity is masked.

insulation properties (Fig. 5), the performances of semi-closed cell foams surpass those of the open cell foam MEL as expected. One may note however that locally around 550 Hz, the sound transmission loss of the SC2 is comparable to that of the MEL. This is due to a half wavelength compression resonance in the material thickness, estimated theoretically at 400 Hz.

On the other hand, the two composite porous materials present interesting properties for both absorption and insulation purposes. As far as sound absorption is concerned, the properties of the composite porous materials largely exceed those of the semi-closed cell foams from frequencies 60 Hz and above. In fact, these materials present properties which are close or even better at low frequency compared to those of the MEL foam. The STL-*n* values of composite porous materials are larger than those of the open cell foam. These values are close to the values obtained for the semi-closed cell foam SC2 and slightly lower than those obtained for SC1.

As a summary, the two composite porous materials designed here fulfill the combined properties of enhanced sound absorption properties together with good sound insulation performances. Note that this is fulfilled for frequencies which go beyond the upper frequency limit of the present study.

6 DESCRIPTION OF THE PLATE/ CAVITY EXPERIMENTAL SETUP

Once optimized, the performances of composite porous materials are tested in conditions which are closer

to a realistic sound field encountered in noise enclosures. For this, simulation results obtained using the complete finite element model described above are compared with measurement data obtained with the setup shown in Fig. 5. The overall disposition of the setup closely follows that of the model described above and the dimensions are those reported in Fig. 1.

A large rigid baffle is built using wooden laminate plates (white parts of the floor in Fig. 5). The five walls' cavity is built with highly dense, painted wooden panels. The cavity is surrounded with thick layers of glass wool to reduce the possible contributions of the sound going through the walls and through the baffle. The entire cavity is positioned so that the plate level corresponds to that of the rigid baffle. The condition of simple support is ensured using the mounting system depicted schematically in the insert of Fig. 5.

The sound source is provided using a boomer loudspeaker connected to a hose whose ending is mounted flush in a corner of the cavity. The acoustic flow rate of the source is measured using two microphones mounted flush in a straight portion of the tube. This allows for the determination of the monopole flow rate delivered to the cavity at each frequency of the spectrum examined. Preliminary measurements showed that the setup ensures a good signal to noise ratio at frequencies as low as 80 Hz and up to 600 Hz. The sound field which is radiated by the plate is measured in an anechoic room using a sound intensity probe in the close vicinity of the plate surface. The intensity is measured in the direction normal to the plate surface. By integrating the measured intensity over the grid spanned, the sound power radiated (SPR) by the plate could be computed.

7 RESULTS FOR SOUND PACKAGES INSIDE THE PLATE/CAVITY SYSTEM

This last section makes the appraisal of the single porosity and composite porous materials as described above for controlling the sound power radiated outside the plate/cavity system. Only results obtained when the treatment is placed in front of the plate are discussed here. The porous materials are all modeled using poroelastic elements, that is including the porous frame deformations. In all cases discussed below, a small air gap (3 mm) is left between the plate and the poroelastic material. This configuration is hereinafter referred to as "unbonded".

Note that the validation of the finite element model of the complete plate/cavity system has been presented in Ref. 7 and is not discussed here.

7.1 Experimental Evidence for Double Porosity Materials

As a preliminary result, this first paragraph illustrates the poor sound insulation provided by double porosity materials based on perforated porous materials. Experimental data of sound power radiated by the plate/cavity system are compared for three types of sound packages based on porous materials. The first sound package considered here is made up with 8 cm thick mineral wool, referred to as "single porosity" material. This mineral wool has been chosen because of its low permeability, which makes it a good candidate for the application of the double porosity concept. The mineral wool main properties are: volumic mass of 156 $kg.m^{-3,}$ an air flow resistivity of 88 400 $N.s.m^{-4}$, and a porosity of 0.97.

The second sound package is made up with the previous mineral wool which has been perforated according the double porosity concept to achieve increased sound absorption properties in the frequency range from 100 Hz to 600 Hz. Practically, this solution has been realized associating two layers of 4 cm thick mineral wool, accordingly perforated and for which the perforations have been aligned. This solution is referred to as "Double poro 4 cm + Double poro 4 cm". For this material, the perforations were circular with diameter 45 mm and the meso-porosity was set to 20.2%.

The third solution has been obtained from the previous double porosity treatment by replacing the perforated layer of mineral close to the plate by a non-perforated layer of the same mineral wool. This solution is referred to as "Double poro 4 cm + Single poro 4 cm". This solution was proved numerically and experimentally in impedance tube conditions, to present sound absorption properties which are comparable to that obtained for the double porosity material made from two perforated layers. Therefore the main difference between the two latter treatments lies in the perforation profile along the thickness direction.

Results from experimental data are shown in Fig. 6 where the SPR measured when there is no treatment is also indicated. Note that these configurations have not been implemented because of computational resource limitations when discretizing the perforations with finite elements. Therefore only, experimental data are shown in this paragraph. Finally, the third octave band values are also indicated in the same graph, for which a +10 dB shift has been applied for illustration purposes. This is however of minor importance for the discussion here which concerns mainly the respective hierarchy of the performances rather than the absolute value of the radiated powers.

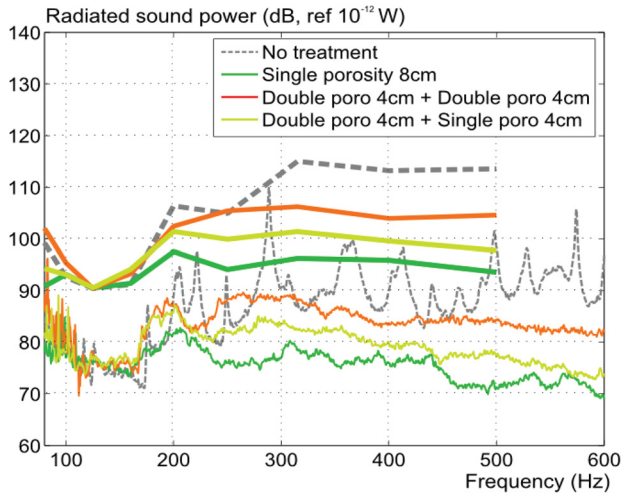

Fig. 6—Sound power radiated by the plate/cavity system treated with single and double porosity materials. The treatments are placed unbonded in front of the plate. Substrate material is mineral wool. Thin lines stands for fine frequency-wise measurement and thick lines indicates third octave band values. Measured data. A + 10 dB shift has been applied to third octave band values for illustration purposes.

These data show that for frequencies below 200 Hz, all treatments provide values of radiated sound power which are comparable to that obtained without treatment. At some frequencies between 150 Hz and 200 Hz, the SPR obtained with double porosity treatments may exceed that obtained without treatment mainly because of the shift of the 200 Hz resonance peaks towards low frequencies.

The picture changes for frequencies above 200 Hz. In this frequency range, all treatments provide a significant noise reduction. The treatment based on the single porosity material provides the largest noise reduction whereas the smallest noise reduction is obtained for the treatment having perforations all through the thickness. Remind that this latter solution present however increased sound absorption properties as measured in impedance tube compared to the single porosity treatment. In addition, the treatment having perforation running along only half of the material thickness provides a noise reduction which is intermediate between the two previous reductions.

The previous observation means that, when the treatment is placed in front of the plate, the noise reduction is not driven by the proportion of sound which is dissipated inside the cavity but rather by the reduction of the sound transmitted through the material. In addition, these data show that the sound transmission performances of double porosity materials based on macro-perforated materials, are mainly governed by the energy transmitted through the perforations.

These experimental results illustrate the need for solutions with increased combined sound absorption and transmission properties. The next paragraph examines the potential of composite porous material for this purpose.

7.2 Treatments Based on Single Porosity Materials

In this section, results for the case when a single porosity treatment is placed unbonded in front of the plate are discussed. These configurations are still the subject of future research and only numerical results are presented here. The three materials described above are tested, namely the open cell foam MEL and the two semi-closed cell foam SC1 and SC2. Results are shown in Fig. 7.

In the frequency range below 200 Hz, the largest noise reduction is provided by the semi-closed cell foams. As expected in this frequency range, the treatment performances are mainly driven by the low permeability of the materials. Above 200 Hz, the performances are mainly driven by the high permeability of the material. Thus, in this frequency range, the largest noise reduction is achieved by the MEL treatment.

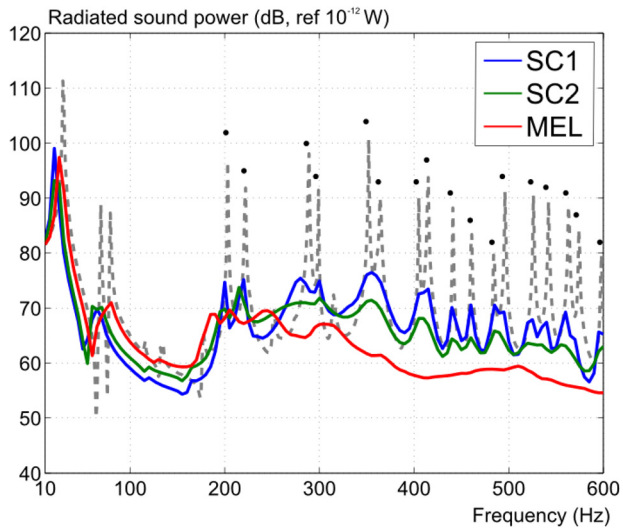

Fig. 7—Sound power radiated by the plate/cavity system treated with single porosity materials. The treatments are placed unbonded in front of the plate. Dashed curved represent the sound power radiated by the plate/cavity system without any treatment. Black dots indicate the positions of the rigid wall cavity modes. Simulated data.

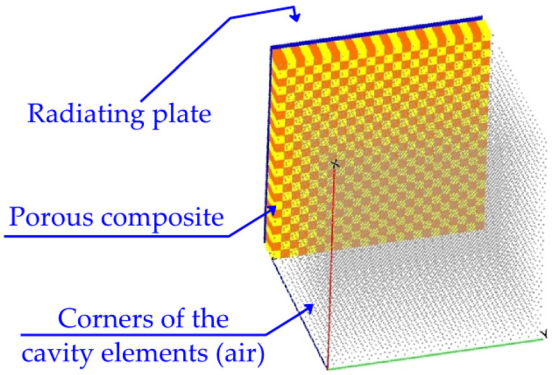

Fig. 8—View of the finite element model of the plate/cavity system. Configuration where the porous composite material is placed in front of the radiating plate.

Overall the entire frequency range, none of the three treatments appears to differ from the other because of too low performances in either of the frequency ranges where the system behavior changes.

7.3 Treatments Based on Composite Porous Materials

This section present the simulated results when the plate/cavity system is treated with composite porous materials (see Fig. 8). Previous results obtained for MEL foam are also indicated as a reference. Results are shown in Fig. 9.

These results show that the noise reductions below 200 Hz obtained with the two composite porous are comparable to those obtained with MEL foam. This may be explained by the fact that the permeability of the composite material is mainly driven by the highest permeability of its components, namely the MEL inclusions. At frequencies above 200 Hz, the increased sound absorption properties of SC1+MEL and SC2 +MEL compared to MEL alone lead to an enhanced noise reduction by 2 to 3 dB.

The results obtained for single porosity and composite porous materials are summarized in Fig. 10 where the radiated sound powers are averaged in third octave bands of frequencies. To emphasize the low frequency behavior of the system, a logarithmic frequency scale is used. As a reference, the sound power radiated when the system is not treated is also indicated.

These results show that, at almost all frequencies, all the treatments provide a significant reduction of the radiated sound power compared to when the system is not treated. In the low frequency range driven by the plate controlled modes, the presence of the SC1 treatment may lead locally to an increase of the radiated

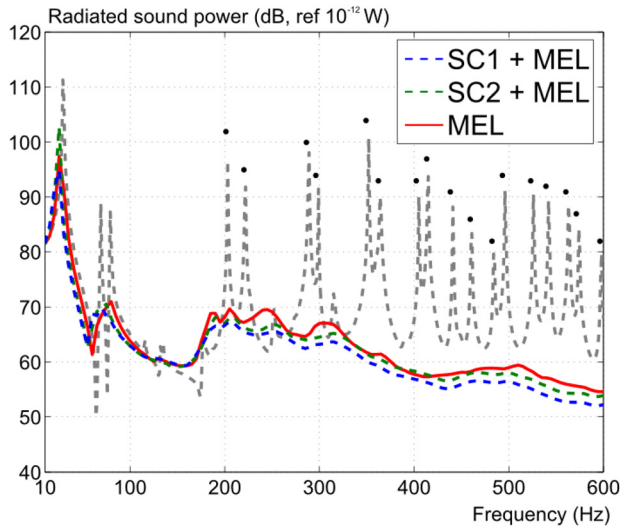

Fig. 9—Sound power radiated by the plate/cavity system treated with composite porous materials (solid lines) and MEL foam (broken line). The treatments are placed unbonded in front of the plate. Dashed curves represent the sound power radiated by the plate/cavity system without any treatment. Black dots indicate the positions of the rigid wall cavity modes. Simulated data.

sound power, mainly by shifting the first plate (1,1) mode to lower frequencies where the dissipation in the system is lower.

Moreover, this graph illustrates the compromise achieved by the composite porous treatments. The performances of these latter solutions are close to those of purely sound insulating materials when vibrational properties are concerned and close to those of purely sound absorbing materials when acoustic dissipation is concerned.

Deeper insights into the physics may be gained by analyzing the dissipated sound powers in the plate and in the poroelastic materials.

7.4 Discussion of the Dissipated Powers

Three types of dissipation may occur in the elements involved here. In the poroelastic treatments, whether single porosity or composite materials, visco-inertial and thermal dissipation may occur. In addition, structural dissipation due to the porous skeleton deformation may also arise. In the plate, only structural deformation may occur. Interested readers are referred to Ref. 27 for the rigorous derivation of the expressions of the dissipated powers in poroelastic materials.

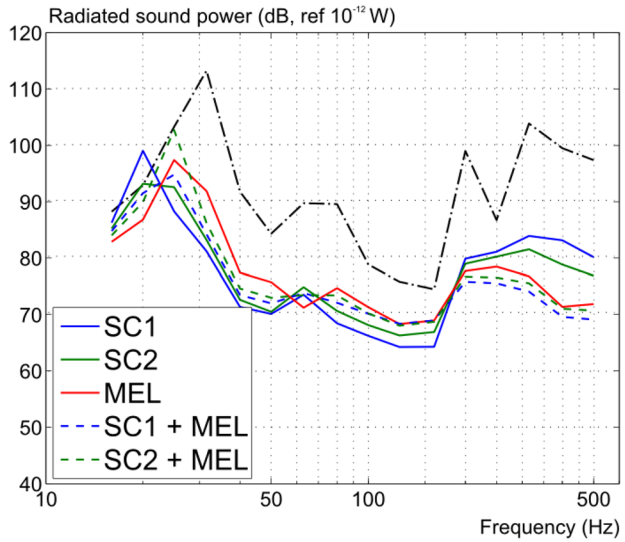

Fig. 10—Sound power radiated by the plate/cavity system treated with all materials. The treatments are placed unbonded in front of the plate.Values are given here in third octave frequency bands and a logarithmic frequency scale is used. Dashed-dotted curves represent the sound power radiated by the plate/cavity system without any treatment. Simulated data.

When comparing different sound packages, a bias may rise in the power balance because the injected powers in the system are different for different sound packages. To overcome this, the dissipated powers examined in the following are normalized by the total dissipated power in the system. Results are shown in Fig. 11 when the system is treated with the MEL foam and in Fig. 12 when the system is treated with the SC1+MEL composite porous. Similar results as those shown in Fig. 12 are obtained with the SC2+MEL treatment shown in Fig. 12.

For the two types of treatments, the visco-inertial dissipation in the porous material is close to 1, which means that this type of dissipation mainly governs the total power dissipated in the system. One could note that below 200 Hz, the SC1+MEL sound package presents a larger visco-inertial dissipation compared to the MEL. This is probably due to the low permeability of the semi-closed cell foam comprised in the composite porous material. For the same reason, the power dissipated by thermal effects for the SC1+MEL solution is much lower than for the MEL material.

Moreover, the power dissipated by structural effects in the porous material is larger in the case of the SC1+MEL material than for the MEL material on the

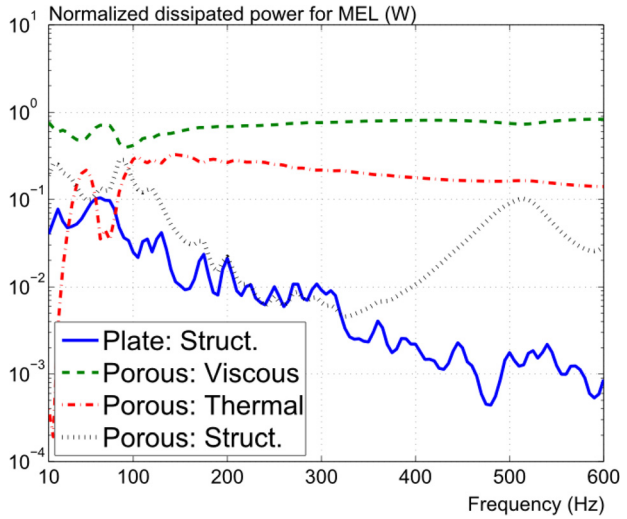

Fig. 11—Dissipated power in the plate/cavity system treated with MEL foam. The treatment is placed unbonded in front of the plate. Simulated data.

entire frequency range observed. In this case, the damping properties of the semi-closed cell foam appear to be determinant. Finally, the dissipated power in the plate is less for the SC1+MEL sound package than for the MEL material. This latter observation proves that the efficiency of the SC1+MEL sound package is effectively due to the enhanced properties of the material.

Finally, it should be underlined that a slightly different picture may be obtained when the treatment is directly bonded onto the plate. As observed in Ref. 6 in this case, the dissipated power at low frequencies is

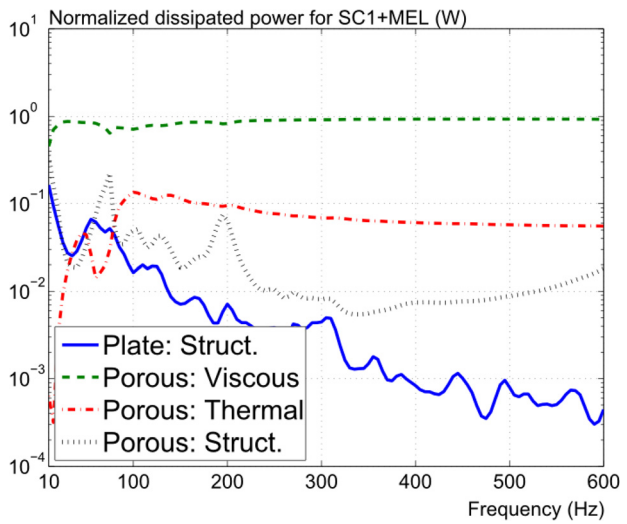

Fig. 12—Dissipated power in the plate/cavity system treated with SC1+MEL composite porous material. The treatment is placed unbonded in front of the plate. Simulated data.

mainly governed by the structural dissipation in the porous layer. Therefore, a larger benefit is expected to show with the composite porous treatment because of enhanced damping properties of the semi-closed cell foams compared to open cell foam. These configurations, which require larger computational resources, are currently under study and will be presented in a future communication.

8 CONCLUSIONS

The study presented here, based on both experimental and numerical data, examines the potential of composite porous materials to achieve increased combined properties of sound absorption and sound transmission. These materials are perforated porous material, the perforations of which are filled with a different porous material. In this respect, composite porous materials may be seen as an extension of double porosity material and may be modeled accordingly.

The composite porous materials have been designed from three materials, two semi-closed cell foams showing good insulation properties and an open cell foam having good sound absorption properties. The properties have been optimized for impedance tube conditions, as if tested according to the corresponding ISO standards. An analytical model has been used to optimize sound absorption and a finite element model to check the sound transmission. The final resulting properties are interesting in the sense that they combine maintained sound insulation with respect to that obtained with the semi-closed cell foam alone and increased sound absorption properties compared to that achieved with the open cell foam alone.

In order to test more realistic sound field conditions, a canonical plate/cavity system representing a typical noise enclosure with an internal acoustic source has been chosen. A finite element model of the complete plate/cavity system has been implemented with poroelastic elements for the treatment of the system. With this model, it has been shown that these composite materials are able to provide a significant reduction of the sound power radiated in the exterior domain on the entire frequency range. The achieved noise reduction is close to that obtained at low frequencies with the semi-closed cell foam alone and better to that obtained with the open cell foam at higher frequencies.

The results presented here show the potential of using composite porous materials to design robust noise control treatment for elaborated configurations. Note that the results presented in Ref. 4 also show that the performances of porous composite materials were maintained when covered by an impervious screen. Taking benefit of a possible optimization of mass and damping, this type of materials may also be of interest in situations where the sound control package is directly connected to the flexible structure. These situations are subject of ongoing research.

9 ACKNOWLEDGMENTS

The authors would like to warmly thank Jean-Baptiste Dupont from LMFA-ECL for his technical assistance during the experiments and Emmanuel Gourdon from ENTPE for the numerical resources. The authors are also grateful to the material manufacturers for providing the samples. This work has been realised in the framework of CAHPAC, a French research projet driven by CNRS and involving beside ENTPE, INRS-Nancy, EC-Lyon, FEMTO-Besançon, IEMN-Lille and LMA-Marseille.

10 REFERENCES

1. X. Olny and C. Boutin, “Acoustic Wave Propagation in Double Porosity Media”, *J. Acoust. Soc. Am.*, **114**, 73–89, (2003).
2. F. Sgard, X. Olny, N. Atalla and F. Castel, “On the use of Perforations to Improve the Sound Absorption of Porous Materials”, *Applied Acoustics*, **66**, 625–651, (2005).
3. F.-X. Bécot, L. Jaouen and E. Gourdon. “Application of the Dual Porosity Theory to Irregularly Shaped Porous Materials”, *Acta Acustica united with Acustica*, **94**, 715–724, (2008).
4. L. Jaouen and F.-X. Bécot “Reinforcement of Acoustical Material Properties Using Multiple Scales”, *SIA Automotive and railroad comfort*, (2008).
5. E. Gourdon and M. Seppi, “On the use of Porous Inclusions to Improve the Acoustical Response of Porous Materials: Analytical Model and Experimental Verification”, *Applied Acoustics*, **71**(4), 283–298, (2010).
6. F.-X. Bécot and F. Sgard, “On the use of Poroelastic Materials for the Control of the Sound Radiated by a Cavity Backed Plate”, *J. Acoust. Soc. Am.*, **120**(4), 2055–2066, (2006).
7. F.-X. Bécot, F. Sgard and N. Amirouche, “Noise Control Optimisation of Machinery Enclosures: Theory, Materials and Experiments”, *Noise at Work*, (2007).
8. N. Atalla, R. Panneton and P. Debergue “A Mixed Displacement-Pressure Formulation for Poroelastic Materials”, *J. Acoust. Soc. Am.*, **104**, 1444–1452, (1998).
9. H.-Y. Lai, “Modeling of Acoustical Properties of Limp Fibrous Materials”, PhD thesis, Purdue University, (1997).
10. R. Panneton, “Comments on the Limp Frame Equivalent Fluid Model for Porous Media”, *J. Acoust. Soc. Am.*, **122**(6), EL217–EL222, (2007).
11. N. Atalla and R. Panneton, “The Effects of Multilayer Sound-Absorbing Treatments on the Noise Field Inside a Plate Backed Cavity”, *Noise Control Engr. J.*, **44**(5), 235–243, (1996).
12. P. Debergue, R. Panneton and N. Atalla, “Boundary Conditions for the Weak Formulation of the Mixed (u,p) Poroelasticity Problem”, *J. Acoust. Soc. Am.*, **106**, 2383–2390, (1999).
13. N. Atalla, M. A. Hamdi and R. Panneton “Enhanced Weak Integral Formulation for the Mixed (u, p) Poroelastic Equations”, *J. Acoust. Soc. Am.*, **109**, 3065–3068, (2001).
14. X. Olny, R. Panneton and J. Tran-van “An Indirect Acoustical Method for Determining Intrinsic Parameters of Porous Materials”, *Poromechanics II, 2nd Biot conference*, (2002).

15. R. Panneton and X. Olny "Acoustical Determination of the Parameters Governing Viscous Dissipation in Porous Media", *J. Acoust. Soc. Am.*, **119**, 2027–2040, (2006).
16. X. Olny and R. Panneton "Acoustical Determination of the Parameters Governing Thermal Dissipation in Porous Media", *J. Acoust. Soc. Am.*, **123**, 814–824, (2008).
17. Y. Champoux and J.-F. Allard "Dynamic tortuosity and Bulk Modulus in Air-Saturated Porous Media", *J. Appl. Phys.*, **70**, 1975–1979, (1991).
18. D. L. Johnson, J. Koplik and R. Dashen "Theory of Dynamic Permeability and Tortuosity in Fluid-Saturated Porous Media", *J. Fluid Mech.*, **176**, 379–402, (1987).
19. D. Lafarge, P. Lemarinier, J-F. Allard and V. Tarnow "Dynamic Compressibility of Air in Porous Structures at Audible Frequencies", *J. Acoust. Soc. Am.*, **102**, 1995–2006, (1997).
20. L. L. Beranek "Acoustic Impedance of Porous Materials", *J. Acoust. Soc. Am.*, **13**, 248–260, (1942).
21. ISO 9053 "Acoustics - Materials for Acoustical Applications - Determination of Airflow Resistance", (1991).
22. H. Utsuno, T. Tanaka, T. Fujikawa and A. F. Seybert "Transfer Function Method for Measuring Characteristic Impedance and Propagation Constant of Porous", *J. Acoust. Soc. Am.*, **86**, 637–643, (1989).
23. C. Langlois, R. Panneton and N. Atalla, "Polynomial Relations for Quasi-Static Mechanical Characterization of Isotropic Poroelastic Materials", *J. Acoust. Soc. Am.*, **110**(6), 3032–3040, (2001).
24. O. Dalinov, F. Sgard and X. Olny, "On the Limits of an "In Vacuum" Model to Determine the Mechanical Parameters of Isotropic Poroelastic Materials", *J. Sound Vibr.*, **276**, 729–754, (2004).
25. F. Sgard, F. Castel and N. Atalla, "Use of a Hybrid Adaptive Finite Element/Modal Approach to Assess the Sound Absorption of Porous Materials With Meso-Heterogeneities", *Applied Acoustics*, **72**(4), 157–168, (2011).
26. "Acoustics - Determination of Sound Absorption Coefficient and Impedance in Impedance Tubes – Part 2: Transfer-function method", International Standard ISO 10534–2: 1991, International Organization for Standardization, (1991).
27. O. Dazel, F. Sgard, F.-X. Bécot and N. Atalla, "Expressions of Dissipated Powers and Stored Energies in Poroelastic Media Modeled by {u,U} and {u,P} Formulations, *J. Acoust. Soc. Am.*, **123**(4), 2054–2063, (2008).